THE JOURNAL OF PHYSICAL CHEMISTRY B

ARTICLE

pubs.acs.org/JPCB

Carotenoid Excited-State Properties in Photosynthetic Purple Bacterial Reaction Centers: Effects of the Protein Environment

Jie Pan,[*,†] Su Lin,[*,†,‡] James P. Allen,[‡] JoAnn C. Williams,[‡] Harry A. Frank,[§] and Neal W. Woodbury[†,‡]

[†]The Biodesign Institute at Arizona State University, Arizona State University, Tempe, Arizona 85287-5201, United States

[‡]Department of Chemistry and Biochemistry, Arizona State University, Tempe, Arizona 85287-1604, United States

[§]Department of Chemistry, University of Connecticut, Storrs, Connecticut 06269-3060, United States

ABSTRACT: Carotenoid excited-state properties are characterized and compared in reaction centers (RCs) of wild-type (WT) *Rhodobacter (Rb.) sphaeroides*, and a mutant VR(L157), in which the near-infrared absorbance band associated with the primary electron donor, P, is missing. Energy transfer from the carotenoid (spheroidenone) S_2 and relaxed S_1 excited states to an adjacent monomeric-bacteriochlorophyll is unchanged between WT and the mutant RC samples. However, two other excited states, including a vibrationally hot S_1 state and a state referred to as S*, have distinct properties in the two RCs. The lifetime of the hot S_1 state is significantly shortened in the P-less mutant compared to WT RCs (450 fs vs 800 fs, respectively), and there is a nearly 2-fold decrease in the efficiency of energy transfer from the carotenoid to bacteriochlorophyll in the P-less mutant relative to WT RCs. The fact that both the observed hot S_1 excited state lifetime and the energy transfer efficiency decrease in the mutant implies that the intrinsic lifetime of the hot S_1 state in the P-less mutant has decreased. Interestingly, the S* state is observed only in the P-less mutant, and it is not present in the WT. The change in the hot S_1 lifetime between WT and mutant RCs, and the formation of the S* state only in the mutant, suggests that the carotenoid binding pocket in the P-less mutant is substantially altered. The excited-state behavior of spheroidene in WT RCs isolated from anaerobically grown cells was also characterized and compared with previous studies of spheroidene in the light-harvesting complex II (LH2) from *Rb. sphaeroides*. Differences in the photophysical properties of spheroidene between WT RCs and LH2 parallel those observed for spheroidenone between WT and VR(L157) mutant RCs. On the basis of the structural information available for both RCs and LH2, it appears that the hot S_1 state and the S* state are sensitive to the structural constraints imposed by protein−carotenoid interactions. Finally, in the VR(L157) mutant, it is possible to directly observe the carotenoid triplet state, likely formed via quenching of the bacteriochlorophyll triplet state. This provides direct experimental evidence for triplet energy transfer to the carotenoid, a process that is integral to the photoprotective role of carotenoids in bacterial RCs.

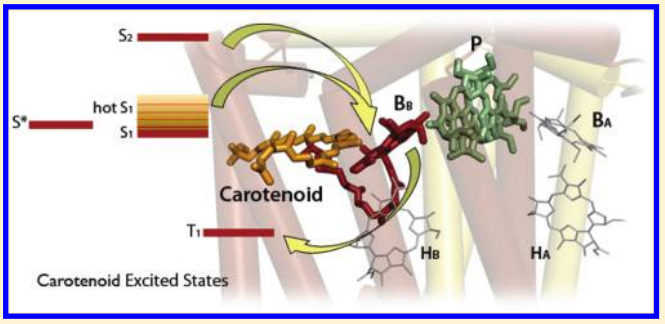

INTRODUCTION

Carotenoids are key elements essential for photosynthetic complexes. They harvest light in a spectral region where chlorophylls/bacteriochlorophylls have only weak absorbance, and they transfer the energy to the photosynthetic apparatus. Under intense light conditions, carotenoids participate in light energy regulation and photoprotection processes.[1] The complexity of carotenoid excited states underlies their versatile functional roles in various pigment−protein systems. So far, our understanding of carotenoid photophysics comes primarily from studies of carotenoids in solution and in various light-harvesting complexes (for reviews, see refs 2−4). Those studies have suggested that interactions of carotenoids with the surrounding environment are crucial in determining carotenoid properties either in solution or when bound to a protein. However, in contrast to numerous experiments which have varied solvent properties such as polarity,[5−7] systematic studies to interrogate the effects of the protein environment on carotenoid excited states are rare and challenging to perform. This is due, in part, to the scarcity of structurally characterized carotenoid−protein systems in which the protein environment can be systematically perturbed and the carotenoid spectroscopy can be specifically monitored.

The photosynthetic reaction center (RC) of purple nonsulfur bacteria contains a single carotenoid,[8] making it a particularly interesting system for the study of carotenoid−protein interactions. The RC protein complex is composed of three subunits (H, L, and M), and cofactors including four bacteriochlorophylls, two bacteriopheophytins, two quinones, a nonheme iron, and a carotenoid.[9] These cofactors are arranged into two symmetrical groups, referred to by the subscripts A and B (Figure 1). The function of RCs is to convert light energy into *trans*-membrane chemical potential through a series of electron transfer reactions initiated from a pair of bacteriochlorophylls, P, proceeding only

Received: January 4, 2011
Revised: March 22, 2011
Published: April 13, 2011

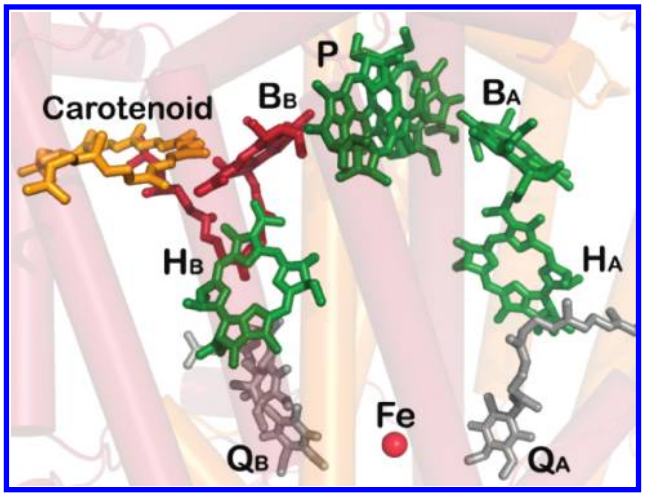

Figure 1. Protein structure of the WT photosynthetic RC from *Rb. sphaeroides* in its neutral state (PDB code: 2J8C). The primary electron donor, P, which is a pair of bacteriochlorophyll (BChl) molecules, and the monomer-BChl on the A side, B_A, as well as bacteriopheophytins at both sides, H_A and H_B, are shown in green. The monomer-BChl on the B side, B_B, is shown in red. In the case of B_B, the phytol tail is shown, but not for the other bacteriochlorins. The 15, 15′-*cis*-configuration carotenoid is shown in orange. Two quinone molecules, Q_A and Q_B, are shown in gray, and the nonheme iron is represented by a red ball.

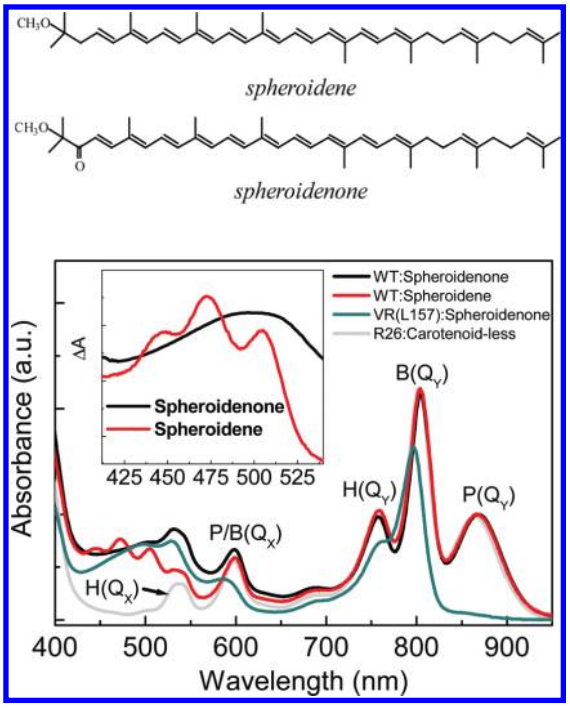

Figure 2. Upper: Molecular structures of spheroidene and spheroidenone. Lower: Absorption spectra of samples from WT *Rb. sphaeroides* RCs containing spheroidenone (black line), WT RCs containing spheroidene (red line), the VR(L157) mutant containing spheroidenone (dark cyan line), and a carotenoid-less mutant, R26 (gray line). Each of the major absorption bands of bacteriochlorins cofactors is labeled. The spectra of the two types of WT RC and the R26 samples were normalized at the spectral peak of the primary electron donor, P, at 865 nm. The spectrum of the VR(L157) RC sample was scaled to match the signal intensity of the spheroidenone-containing WT sample in the carotenoid absorption region. The inset shows difference spectra representing the apparent in situ absorption of the two types of carotenoids involved in this study, obtained by subtracting the absorption spectrum of carotenoid-less R26 RCs from the corresponding carotenoid-containing absorption spectra.

along the A branch.[10] The carotenoid in the RCs of purple bacteria such as *Rb. sphaeroides* is unusual in that it is maintained in a *cis*-configuration in the binding pocket. In addition, the detailed interactions with the protein are distinct from those of the more extensively investigated light-harvesting complex II (LH2).[8,11,12] The RC carotenoid is thought to play a major role in photoprotection.[1] The triplet excited state of P, formed by charge recombination, can interact with oxygen to form singlet oxygen. The carotenoid presumably quenches triplet P as a result of triplet−triplet energy transfer via the B-side monomer bacteriochlorophyll molecule, B_B,[13] although formation of the resulting triplet carotenoid has never been directly observed in RCs. When excited directly, the RC carotenoid can also undergo singlet energy transfer to B_B,[14,15] which is in van der Waals contact with the carotenoid.[8] In addition to having a single carotenoid, the RC is easily manipulated genetically, and many mutants are available including a number that affect the protein environment of the various cofactors.[16,17]

Carotenoids have a complex excited state manifold which includes S_1 and S_2 states, a vibrationally unequilibrated ("hot") S_1 state[18−23] and a state denoted as S* (for a review, see ref 24). In addition, there is a theoretically predicted, but experimentally ambiguous $1B_u^-$ state.[24−26] Both the S_2 and relaxed S_1 states are well documented.[2] The absorption of carotenoids in the 450−550 nm spectral region arises from the strongly allowed $S_0 \rightarrow S_2$ transition, while the transition from S_0 to the S_1 state is symmetry forbidden due to optical selection rules. The S_2 state is extremely short-lived, and relaxes to the S_1 state through internal conversion within a few hundred femtoseconds. The S_1 state is a more stable state with a lifetime that varies from a few picoseconds to tens of picoseconds. Both S_2- and relaxed S_1-state-mediated excitation energy transfers (EETs) from carotenoids to nearby chlorophyll/bacteriochlorophyll molecules have been identified in various light-harvesting complexes.[2,3,27] However, the properties and functional roles of the hot S_1 and S* states are still controversial.

Here, femtosecond transient absorption spectroscopy is used to characterize carotenoid excited state properties in RCs from wild-type (WT) *Rb. sphaeroides* and a mutant, VR(L157), in which the replacement of valine with arginine at residue L157 near the special pair results in the disappearance of the 865 nm absorbance band (Figure 2), due to the partial or complete loss of P.[28] In addition, WT RCs prepared with two different carotenoids (spheroidenone and spheroidene) are investigated. Our results indicate that the protein environment plays a major role in shaping the carotenoid excited state manifold in bacterial RCs.

MATERIALS AND METHODS

Sample Preparation. WT RCs from *Rb. sphaeroides* were expressed with a polyhistidine (Poly-His) tag, as described previously.[29] Cells were grown either anaerobically under the illumination of a 150 W high-pressure sodium lamp (resulting in spheroidene as the carotenoid), or semiaerobically in the dark (in which case they contain spheroidenone). Detailed procedures for the purification of RCs with poly-His-tags are described in ref 30. Construction and expression of the mutant VR(L157) RCs, and

their isolation, have been described previously.[28] All RC samples were suspended in 50 mM Tris-HCl (pH 8.0), 0.025% LDAO, 1 mM EDTA.

Laser Spectroscopy. Femtosecond transient absorption measurements were performed using a system based on a kilohertz Titanium:Sapphire laser. Briefly, laser pulses of 1 mJ, at a repetition rate of 1 kHz (100 fs pulse duration at 800 nm), were generated from a regenerative amplifier system (Tsunami and Spitfire, Spectra-Physics). Part of the pulse energy ($\sim$ 200 μJ) was used to pump a home-built, noncollinear optical parametric amplifier (NOPA) to generate 495-nm excitation pulses, following a similar design in ref 31. The broad-band probe pulse was generated by focusing a weak 800-nm beam into a 3-mm sapphire plate, and sent to an optical compressor composed of a pair of prisms (CVI), before it was focused onto the sample. The white-light probe pulses were then dispersed by a spectrograph and detected, shot-by-shot, using a charge-coupled device (CCD) camera (DU420, Andor Technology). The collected data had a $\sim$ 2.3 nm spectral resolution. The polarization of the pump pulses was set to the magic angle (54.7°) with respect to that of the probe pulses. For WT RC measurements, samples were contained within a 2-mm path-length cuvette mixed by a magnetic stir bar, and the absorption at 800 nm was 0.8−1.0. The primary electron donor, P, was accumulated in the oxidized state through constant illumination by both the 495 nm pump beam and background illumination at 800 nm. This is made possible by the fact that the charge-separated state, $P^+Q_A^-$, lives for 100 ms. For measurement of the VR(L157) mutant, samples were loaded into a spinning-wheel with an optical path-length of 1.2 mm. All of the experiments were performed at room temperature.

Data Analysis. The recorded time-resolved spectra were analyzed either with a global analysis program provided by Dr. Mikas Vengris at Vilnius University, Lithuania,[32] or a locally written program, ASUFIT. [www.public.asu.edu/~laserweb/asufit/asufit.html] The instrument response function was fit to a Gaussian curve (full-width at half-maximum of 100 − 120 fs) and the group velocity dispersion of the white light probe pulse was fitted to a third-order polynomial.

RESULTS

Ground state absorption spectra of WT RCs containing either spheroidene or spheroidenone and VR(L157) mutant RCs containing spheroidenone are shown at the bottom of Figure 2. The chemical structures of these two carotenoids are shown at the top of Figure 2. Spheroidene is the primary carotenoid in cells grown under anaerobic conditions, while spheroidenone, with an additional carbonyl group, predominates in cells grown under semiaerobic conditions. Dark, semiaerobic growth is preferable for cells with mutant RCs in order to avoid reversion (back to WT) under photosynthetic selection. The absorption spectra of spheroidene- and spheroidenone-containing WT RCs are nearly identical in the spectral region between 700−900 nm, but significant differences can be seen in the carotenoid $S_0 \rightarrow S_2$ transition region from 420 to 525 nm. The inset of Figure 2 shows the absorption spectra calculated for spheroidene and spheroidenone in the RC, obtained by subtracting the absorption spectrum of carotenoid-less R26 RCs[15] (Figure 2 gray curve) from the corresponding carotenoid-containing RC spectrum. The absorption spectrum of spheroidene shows vibrational structure in the $S_0 \rightarrow S_2$ transition region, while spheroidenone

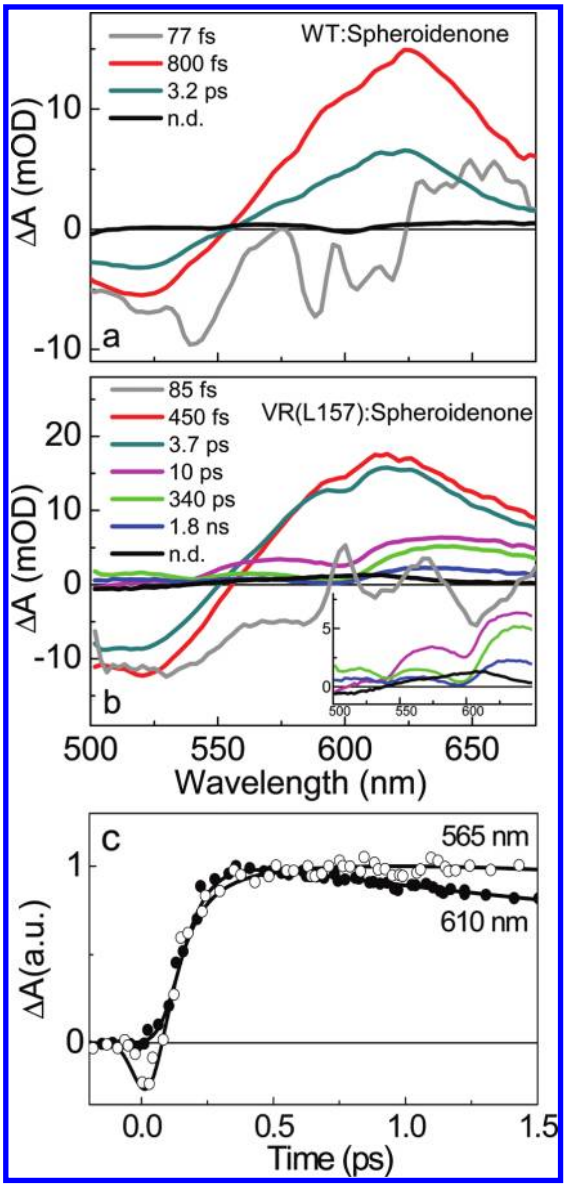

Figure 3. (a) EADS from a global analysis using a sequential model in the 500−680 nm region upon 495 nm excitation of WT *Rb. sphaeroides* RCs containing spheroidenone, in which the primary electron donor is oxidized forming P^+. (b) VR(L157) mutant RCs containing spheroidenone (excitation conditions as in panel a). Inset: Enlargement of the last four EADS. Each respective EADS evolves into the next with the given time constant. The final component is nondecaying (n.d.). (c) Normalized kinetic traces recorded at probe wavelengths of 565 nm (open circles, ○) and 610 nm (filled circles, ●), respectively, for the spheroidenone-containing VR(L157) RC samples after excitation at 495 nm. Solid lines represent the fitting result using global analysis with a sequential model.

exhibits only a single, broad absorbance band that is red-shifted due to the increased π−electron conjugation length provided by the additional carbonyl group.[2] For VR(L157) RC samples, the spectral profiles in the bacteriopheophytin and monomer bacteriochlorophyll absorbance regions are comparable to those of WT RCs. However, the 865-nm band is missing in the mutant, and the 600-nm band is smaller and blue-shifted. Together with the significantly decreased Soret band intensity at ~400 nm (data not shown), this argues that at least one, and probably both, of

the bacteriochlorophyll molecules that form P in WT RCs are lost in the VR(L157) mutant.[28] The carotenoid absorption region is similar in spheroidenone-containing VR(L157) and WT RCs, indicating that the carotenoid is intact in the mutant RC.

Excited States of Spheroidenone in WT versus VR(L157) RCs. Femtosecond transient absorption measurements were performed using direct excitation of the carotenoid S_2 state at 495 nm, and probing over a broad wavelength region from 475 to 950 nm. Transient absorption spectra of WT and VR(L157) mutant RCs, both containing spheroidenone, were recorded over a time range extending from 0.5 ps before to 7 ns after the excitation pulse. Global fitting was used to analyze each data set in the spectral region from 475 to 680 nm, using a sequential, irreversible, kinetic model (A → B → C → D...). While this does not necessarily result in spectra representing pure intermediate states, it provides a simple means of dissecting the progression of spectral changes. The spectral profiles obtained from such an analysis are called evolution associated decay spectra (EADS).[33] For WT, spheroidenone-containing RCs, four components were resolved with exponential decay lifetimes of 77 fs, 800 fs, 3.2 ps, and a nondecaying component (Figure 3a). Three additional components are required for an adequate fit of the data from the VR(L157) mutant (Figure 3b). Seven components is a large number of fitting parameters. However, kinetically these components are reasonably well separated, being spread over nearly 4 orders of magnitude in time due to the very long-lived states in the mutant.

Initial Carotenoid Excited States. The first (shortest time scale) EADS for both RC samples (gray curves in Figure 3a,b) represents the initially excited S_2 state of spheroidenone. It contains mainly broad, negative absorbance changes due to ground-state bleaching and stimulated emission from the S_2 state. The lifetime of the first EADS is the same within experimental error in both WT and VR(L157) mutant RCs (<100 fs). As the first EADS evolves into the second one, a broad positive band appears, peaking at 620 and 610 nm in WT and the VR(L157) RCs, respectively. Such a strong positive absorption band in the visible spectral region is typically attributed to the carotenoid $S_1 \rightarrow S_N$ transitions,[2,27] indicating formation of the carotenoid S_1 state. The lifetime of this S_1-state is 800 fs in WT RCs and 450 fs in the VR(L157) mutant RCs.

Vibrational Relaxation of the S_1 State. The third EADS for each sample (dark cyan curves in Figure 3a,b) also exhibits the spectral features of a carotenoid S_1 state, but the lifetime is longer. In this case, the decay kinetics are about the same for WT and the VR(L157) mutant (3.2 and 3.7 ps, respectively). This kinetic progression from an initial S_1 state that is short-lived (the second EADS of Figure 3a,b) to a final, longer-lived state (the third EADS of Figure 3a,b) has been seen previously and interpreted as the evolution from a vibrationally excited or "hot" S_1 state to a relaxed S_1 state.[2,18,23,27,34,35] The subpicosecond lifetime of the initial S_1 state observed here is consistent with that seen in previously studied systems. Previous measurements have also shown a blue shift of the $S_1 \rightarrow S_N$ transition band between the relaxed and hot S_1 states. In Figure 3a,b, the second and the third EADS have very similar spectra, but this is not too surprising; these spectra are very broad, and potentially mixed with excited state spectra from B_B, as discussed later. A small amplitude decrease on the red side of this band would be difficult to observe. The blue shift is much more easily observed in spheroidene-containing RCs, as the spectral features are much sharper

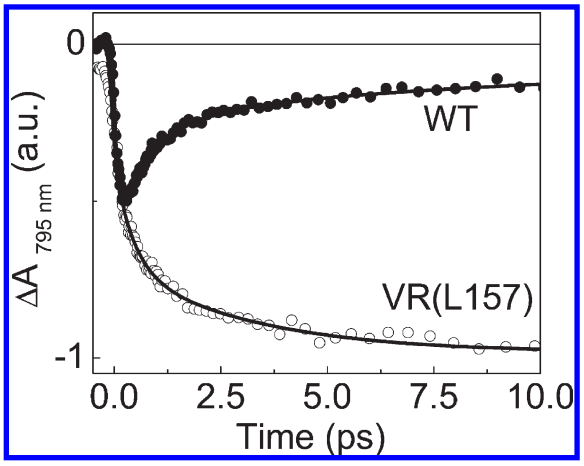

Figure 4. Normalized kinetic traces recorded at a probe wavelength of 795 nm for spheroidenone-containing RC samples from WT (filled circles, ●) and the VR(L157) mutant (opened circles,○), upon excitation at 495 nm. The amplitude of the WT trace is scaled to half of that for the VR(L157) mutant (see text for details). The solid lines represent fitting curves.

(this is discussed below in the section on spheroidene-containing RCs). However, a careful look at the early time kinetics gives a clearer picture. This is shown in Figure 3c for the VR(L157) mutant. The absorbance change at 565 nm on the blue side of the $S_1 \rightarrow S_N$ transition increases and then continues to climb slowly over the course of the first picoseconds. In contrast, the red side of the $S_1 \rightarrow S_N$ transition increases rapidly and then decreases. This is what one would expect for a blue shift of this band during the relaxation process.[18] The kinetics associated with the relaxation are difficult to see in WT RCs because on the same time scale B_B^* is decaying due to an interaction with P^+ (see below). These observations suggest that the second EADS represents a hot S_1 state of spheroidenone in both RCs samples. This assignment is supported by data from WT RCs containing spheroidene, which has a more highly resolved spectrum and thus a more pronounced amplitude decrease on the red side of the $S_1 \rightarrow S_N$ transition band (see below).

Energy Transfer from Carotenoid Excited States. Previous work has shown that carotenoids can undergo singlet excited state energy transfer to B_B in the RC.[14,15] Note that measurements in ref 14 were performed using WT RCs in which P was in its neutral state, while P is the oxidized state (P^+) in the current study. Energy transfer yields from carotenoid excited states to B_B are not expected to be affected by the status of P, while decay of the B_B^* state does depend on the presence of redox states of P (see below, and details will be reported elsewhere). Consistent with this, the observed lifetimes of both the S_2 and the relaxed S_1 states of spheroidenone in WT and VR(L157) RC samples (Figure 3a,b) are considerably shorter than those reported for all-*trans*-spheroidenone in solvent at room temperature.[19,34] Since no significant changes in the S_2 and S_1 state lifetimes were observed among different geometric isomers of analogous carotenoids in solvent at 77 K,[36] where their specific configurations can be maintained, the shortened lifetimes are presumably due to quenching by energy transfer, rather than due to the *cis*-configuration. It is less informative to compare the hot S_1 state lifetimes to those determined from measurements in solution, due to the large range of values reported in solvents with different polarities.[19] However, the amplitude of the ground-state bleaching recovery

provides direct evidence for energy transfer. In WT RCs (Figure 3a, red curve), the large amplitude reduction in the ground-state bleaching signal, which accompanies the decay of the positive $S_1 \rightarrow S_N$ transition, indicates that a significant portion of the hot S_1 state returns to the ground state via an additional channel, presumably energy transfer. Interestingly, the amount of ground-state bleaching recovery upon hot S_1 state decay in the VR(L157) mutant (Figure 3b, red curve) is substantially less than that in WT RCs, which indicates a decreased energy transfer yield from this state in the mutant. When this is coupled to the fact that the lifetime of the hot S_1 state of the VR(L157) mutant is significantly shorter than that of the WT RCs (450 fs vs 800 fs), it suggests that the intrinsic decay rate of the hot S_1 state has decreased in the mutant, rather than the rate of energy transfer.

The Energy Transfer Acceptor. Energy transfer from the excited carotenoid to B_B should be evident in the Q_Y region of the spectrum where B_B absorbs most strongly. Figure 4 shows the kinetic traces of the ground-state bleaching associated with B_B at 795 nm, from spheroidenone-containing WT and VR(L157) RC samples.[28] Indeed, the rapid formation of B_B ground-state bleaching, in both RC samples upon carotenoid excitation, clearly demonstrates energy flow from the carotenoid S_2 state. However, in WT RCs, more than half of the B_B bleaching amplitude recovers within 2.5 ps due to efficient quenching by P^+, making it difficult to monitor energy transfer to B_B from other carotenoid excited states on the picosecond time scale. Note that the amplitudes of the kinetic traces for these two RC samples were scaled in such a way to match only the initial bleaching due to energy transfer from the carotenoid S_2 state, as competing decay processes from B_B^* prevent further accumulation of their population at later time scales in WT RCs. In contrast to the situation in WT RCs, B_B^* lives for nanoseconds in VR(L157) RCs (due to the absence of P), and the multiphasic formation of B_B^* is easily observed. The initial development of B_B^* ground-state bleaching in the P-less mutant occurs in less than 100 fs. This is followed by a subpicosecond and then a few picosecond bleaching component. Multiple exponential fitting of the 795-nm kinetics from VR(L157) returns three rise times of 0.08 ps (50%), 0.5 ps (25%), and 3.7 ps (25%), which closely resemble the decay time constants measured in the visible region for the spheroidenone S_2, hot S_1, and relaxed S_1 excited states, respectively (Figure 3b). This is consistent with energy transfer to B_B from these three excited states.

Notice that the B_B^* state also induces a bleaching in the Q_X region around 600 nm. This signal is shown as a weak dip in the EADS spectra in Figure 3b for the VR(L157) mutant. Meanwhile, in WT RCs, the B_B^* state is quenched rapidly by P^+ as shown in the kinetics of the Q_Y band in Figure 4, therefore the 600-nm dip is less visible in the EADS shown in Figure 3a.

A Long-Lived Carotenoid Excited State in VR(L157) RCs Similar to the So-Called S State.* In VR(L157) RCs, there are three additional long-lived EADS required to accurately represent the data, beyond the three described above. These involve broad positive absorption changes that remain in the visible region after the carotenoid S_1 state signal has decayed (lifetime 3.7 ps) (Figure 3b). Specifically, the fourth to sixth components have lifetimes of 10 ps, 340 ps, and 1.8 ns, respectively. On the basis of the 795-nm kinetics of B_B bleaching described above, and from previous studies of the long-lived bacteriochlorophyll excited states in VR(L157) RCs, it is clear that there are long-lived states involving B_B that persist on these time scales. However, the evolution of the 10-ps EADS to the next 340-ps EADS primarily involves changes in the spectral region below 570 nm (Figure 3b, inset), where carotenoid signals dominate, suggesting that the 10-ps time scale process involves a carotenoid excited state.

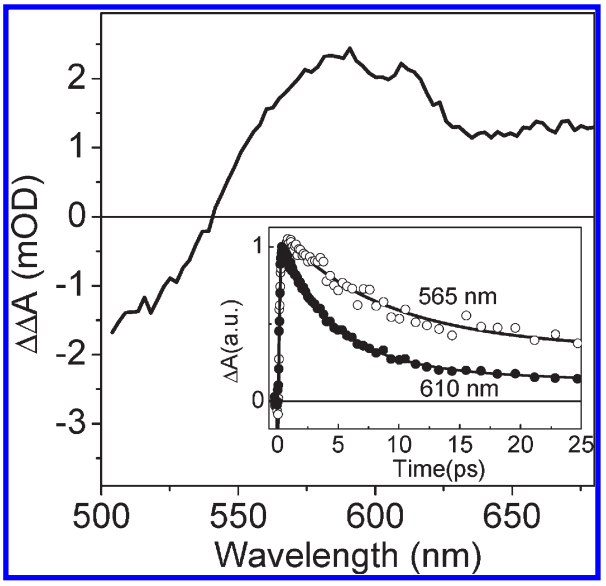

Figure 5. Difference between the fourth and fifth EADS, shown in Figure 3b, with associated lifetimes of 10 and 340 ps, respectively, resulting from global analysis of transient absorption data recorded for VR(L157) RCs. Inset: Normalized kinetic traces recorded at probe wavelengths of 565 nm (open circles, ○) and 610 nm (filled circles, ●), respectively, for the spheroidenone-containing VR(L157) RC samples after excitation at 495 nm. Solid lines represent the results of a fit using global analysis with a sequential model.

In an attempt to remove the B_B contribution to the fourth EADS, and better visualize the nature of any carotenoid state that might be evolving on this time scale, a difference−difference spectrum was generated by subtracting the fifth EADS from the fourth (without normalization). The resulting spectrum shows a positive band peaking at 585 nm and a negative band in the <540 nm region, as one would expect for a carotenoid excited state (Figure 5). The positive absorption band in the difference spectrum in Figure 5 is blue-shifted with respect to the $S_1 \rightarrow S_N$ transition (585 nm, Figure 5, vs 610 nm, Figure 3b), and the lifetime of this signal is longer than that of the S_1 state (10 ps vs 3.7 ps). Both the spectral and dynamic features of this signal are consistent with that of the so-called S* state, as observed in previous studies of carotenoid in light-harvesting complexes and of carotenoids in solution.[19,21−23,35,37] The existence of this S*-like state in VR(L157) mutant RCs (but not in WT RCs) can be further visualized in the comparison of the kinetics at 610 and 565 nm discussed above, except over a 25-ps time window (inset in Figure 5). The signal at 610 nm decays on the same time scale as the carotenoid S_1 state (Figure 3b), while the signal at 565 nm decays more slowly. A similar comparison for spheroidenone in WT RCs shows overlaid kinetic traces at these two probe wavelengths (data not shown), which is consistent with the fact that the spectral shapes for the $S_1 \rightarrow S_N$ transition in the second and third EADS are essentially the same in WT RCs, again implying that no S* state is formed in WT (Figure 3a). Thus, there are spectral and kinetic signals indicative of a possible S* state in the VR(L157) mutant, but not in WT RCs.

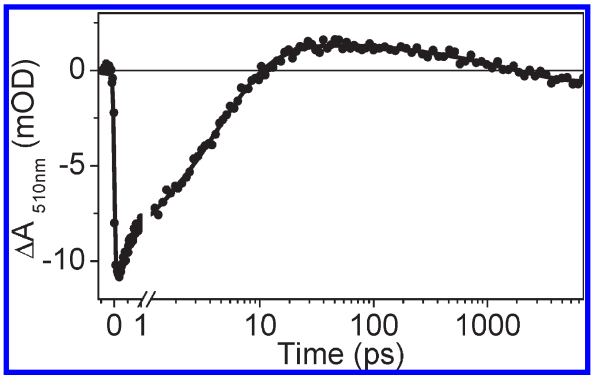

Figure 6. Kinetic trace recorded at 510 nm (filled circles, ●) for spheroidenone-containing VR(L157) RCs after excitation at 495 nm. The solid line represents a fit by global EADS analysis using a sequential model. Note that the time axis is linear until 1 ps and logarithmic to 7 ns.

The above comparison of the spectral and dynamic features of carotenoid excited states reveals similarities and differences between WT and VR(L157) mutant RCs. Energy transfer dynamics from the S_2 and S_1 states are essentially the same for spheroidenone in both WT and the VR(L157) mutant, which implies similar interactions between the carotenoid and B_B in both systems. However, the behavior of the hot S_1 state in terms of observed lifetimes and the yields of energy transfer, and the appearance of signals similar to the previously reported S* state, are distinct between these two RC samples. The carotenoid excited state changes observed in the P-less mutant imply that the coupling and/or interaction of the carotenoid with its environment has been altered, suggesting that the protein environment surrounding the carotenoid has been modified in the mutant, presumably due to the loss of P.

Triplet Carotenoid Formation in the VR(L157) Mutant. There is a nondecaying EADS component in both WT and VR(L157) mutant RC samples in our transient absorption measurements (Figure 3a,b). Although the amplitude of this signal is small, the spectral profiles of the nondecaying component are distinct between WT and the mutant. In WT RCs, the residual signals (over a 100-ps time window) have spectral features associated with the charge-separated state, $P^+H_A^-$, as shown by simultaneous bleaching at 540 and 600 nm.[14] This is presumably due to a residual population of unclosed RCs (a small fraction of RCs in which P is not oxidized). In contrast, the nondecaying EADS component from the VR(L157) mutant, within the 7-ns time window, is comprised of a broad positive band peaking at ~610 nm and a small negative band below 520 nm (Figure 3b inset, black curve). The <520-nm bleaching corresponds to the position of the carotenoid ground state $S_0 \rightarrow S_2$ transition, indicating that this signal is due to a carotenoid state. Figure 6 shows a kinetic trace recorded at 510 nm. The initial bleaching is due to loss of the carotenoid ground state population upon 495 nm excitation, followed by ground-state recovery through energy transfer and decay of the S_1 state. The excited state and charge-separated state of B_B may induce some absorption increase in this region. However, there is an absorbance decrease in this region that continues to build up on the nanosecond time scale, presumably due to carotenoid ground-state bleaching that is reforming on this time scale as the B_B excited state and/or charge-separated state decays. Given the fact that carotenoid singlet states live for less than tens of picoseconds, it is likely that this long-lived signal is due to the carotenoid triplet state, which lives for hundreds of nanoseconds to a few microseconds.[38−40] In WT RCs, no triplet state carotenoid is observed (nanosecond time scale measurements were performed but are not shown). This is because B_B^* in WT RCs is rapidly quenched by P^+, and never undergoes intersystem crossing and triplet−triplet energy transfer.

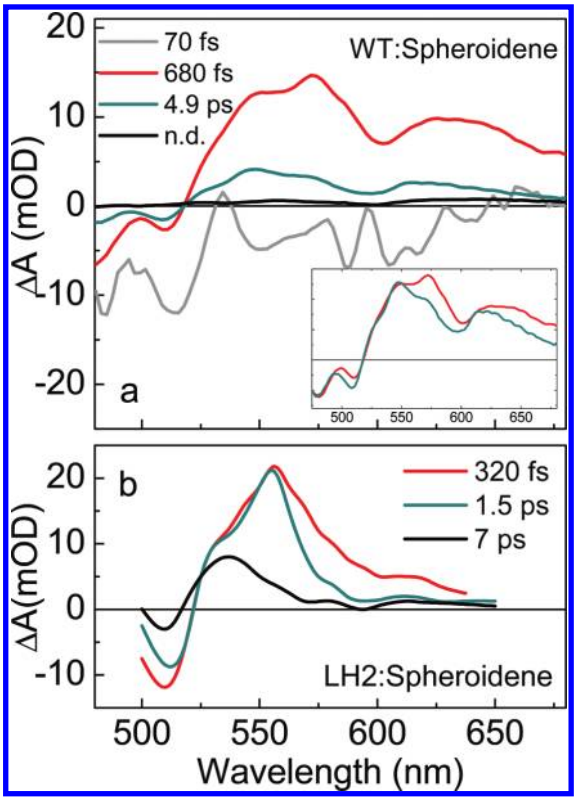

Figure 7. (a) EADS resulting from global analysis using a sequential model in the 475−680 nm region upon 495 nm excitation of 15,15′-*cis*-spheroidene-containing WT RCs with an oxidized primary electron donor, P^+. The inset shows comparison of the second and third EADS; the two curves are normalized on the blue side of the spectra. (b) EADS and associated lifetimes for the all-*trans*-spheroidene in the LH2 complex of *Rb. sphaeroides* upon spheroidene excitation, generated from Figure 2 of ref 23 with permission. For clarity, the initial (<100 fs) component and the last two longer-lived components (70 ps and 2 ns components) in the original LH2 figure are not shown, as they are not needed for this data comparison.

Excited States of Spheroidene in WT RCs. To further understand carotenoid excited state properties in RCs, spheroidene-containing WT RCs were investigated. Spheroidene is one of the most extensively characterized carotenoid species, both in solution and in light-harvesting complexes.[19,23,34,36,41,42] In addition, the spectral features of *cis*-configured carotenoid excited states are better resolved in spheroidene, than in spheroidenone (Figure 2, top), removing some of the interpretation ambiguities associated with analyzing spectral changes.

Global analysis results of the transient absorption spectra recorded for spheroidene in WT RCs upon excitation at 495 nm are shown in Figure 7a. The characteristics of carotenoid excited state properties in all RC samples are compared in Table 1. As seen for spheroidenone in WT RCs, four EADS components generate a satisfactory fit for spheroidene-containing RCs. The first EADS (gray curve), decays in less than 100 fs, and

Table 1. Comparison of the S_2, Hot S_1, S_1, and S* State Lifetimes of Spheroidene and Spheroidenone in RCs from WT, the VR(L157) Mutant, and in the LH2 Complex from *Rb. sphaeroides*, as Well as Measurements for Central-*cis*-spheroidene in Solvent at 77 K[a]

					hot S_1 state				
carotenoid	pigment–protein complex	solvent[b] (77K)	τ_{S2} (fs)	τ_{S1} (ps)	τ_{Obs} (fs)	ϕ_{EET}[c]	τ_{Int}[d] (ps)	τ_{S^*} (ps)	references
central-*cis*-	WT RC		77	3.2	800	45%	1.4		this work
spheroidenone	VR(L157) RC		85	3.7	450	25%	0.6	11	this work
central-*cis*-spheroidene		EPA	120	8.2			0.7		ref 36
	WT RC		70	4.9	680	60%	1.7		this work
all-*trans*-spheroidene	LH2		90	1.5	320	25%		7.0	ref 23

[a] Energy transfer yields (ϕ_{EET}) and estimated intrinsic lifetimes of the hot S_1 state are also listed. [b] EPA, ether/isopantane/ethanol, 5/5/2, v/v/v, from ref 36. [c] ϕ_{EET} from the hot S_1state was estimated from the amplitude of the carotenoid ground-state bleaching recovery accompanying decay of this state. [d] The intrinsic lifetimes (τ_{Int}) were calculated according to $\phi_{EET} = (1 - (\tau_{Obs})/(\tau_{Int})) \times 100$.

represents the initial S_2 excited state absorbance changes. The decay of this EADS is significantly faster than relaxation of the S_2-state of spheroidene in solution.[19] This is indicative of S_2-mediated energy transfer in the spheroidene-containing WT RCs, as was observed for the spheroidenone-containing RCs (both WT and mutant) described above. The second EADS in Figure 7a (red curve) has a lifetime of 680 fs, similar to that observed for spheroidenone-containing WT RCs (Figure 3a). Evolution of the second to the third EADS shows an amplitude decrease of ~60% for both the positive band and the negative ground-state bleaching signals, indicating a high yield of energy transfer from this state, similar to observations in spheroidenone-containing WT RCs. In addition to the overall amplitude changes, a pronounced absorbance decrease on the longer wavelength side of the $S_1 \rightarrow S_N$ transition band is apparent as the second EADS evolves into the third one (Figure 7a). As was the case for spheroidenone-containing RCs, we expect that this is associated with relaxation of a hot S_1 state. The expected spectral change during vibrational relaxation[18,23] is much more obvious in spheroidene-containing RCs (Figure 7a, inset) than it was in spheroidenone-containing RCs (Figure 3a), supporting the assignment of the second EADS as the hot S_1 excited state in WT RCs. Past work has shown that the structure of the carotenoid in bacterial RCs is well-defined. The central backbone region in close contact with the macrocycle of B_B is highly conserved in crystal structures of RCs reconstituted with various spheroidene analogues including spheroidenone.[8] While it is true that in spheroidenone-containing RCs the EADS profiles of the proposed hot S_1 and relaxed S_1 states are similar (Figure 3), it is unlikely that these two kinetically distinct states arise from structural heterogeneity. The third EADS of Figure 7a (dark cyan curve) has a lifetime of 4.9 ps, which is considerably shorter than the 8-ps lifetime found for the same 15,15′-*cis*-spheroidene in solution at 77 K,[36] and again is consistent with substantial energy transfer from the S_1 state of spheroidene in WT RCs.

It is interesting to compare the results for spheroidene in WT RCs with previous measurements in LH2. As was described above for the comparison between spheroidenone-containing WT and VR(L157) RCs, there are differences between spheroidene-containing WT RCs and LH2 in the evolution of the S_1 state (the apparent vibrational relaxation of the hot S_1 state) and the presence of the S* excited state (the initial S_2 excited state dynamics are similar in both systems). For the sake of comparison, three EADS corresponding to the hot S_1, S_1, and S* states of spheroidene in the LH2 complex are plotted in Figure 7b, adapted from Figure 2 of Papagiannakis, et al.[23] In parallel to the WT/VR(L157) comparison, the observed lifetime of the spheroidene hot S_1 state in WT RCs is more than double that observed in LH2 complexes (680 fs vs 320 fs, respectively), and the yield of energy transfer, estimated from the ground-state bleaching amplitude decrease, is significantly higher in WT RCs than in LH2 (60% vs 25%, respectively). Again, this is consistent with a longer intrinsic lifetime of the hot S_1 state in WT RCs than in LH2. The similarity between the P-less mutant and LH2 argues against the idea that the *cis* vs *trans* isomeric difference between the carotenoids in the RC and LH2 gives rise to the different hot S_1 state characteristics. As was the case with spheroidenone, signals associated with the S* state[23,35,37] were not observed in spheroidene-containing WT RCs (Figure 7a). The excited state absorption and ground-state bleaching recovery of the remaining carotenoid signals decay with a time constant of 4.9 ps, which is consistent with the trends described for WT RCs containing spheroidenone, above (Figure 3a). In LH2, the S* state (Figure 7b, black curve) has been detected as an excited state absorption band that is blue-shifted relative to the $S_1 \rightarrow S_N$ transition band of the relaxed S_1 state (Figure 7b, dark cyan curve), and it has a lifetime that is 7 ps, longer than the 1.5-ps lifetime of the relaxed S_1 state. The final nondecaying EADS of spheroidene-containing WT RCs in Figure 7a (black curve) is, again, due to the formation of $P^+H_A^-$ from a small population of unclosed RCs. Therefore, the differences in the carotenoid excited-state properties between spheroidene-containing WT RCs and LH2 are very similar to the differences between spheroidenone-containing WT and mutant VR(L157) RCs.

Spectral Characteristics of *cis*-Configured Spheroidene in Protein. The well-defined central-*cis*-configuration of the single carotenoid found in bacterial RCs provides an ideal platform from which to characterize the excited state spectral features of a *cis*-isomer in a particular protein environment. In contrast to a single band peaking at ~556 nm for the $S_1 \rightarrow S_N$ transition of all-*trans*-spheroidene in LH2 (Figure 7b), a much broader, double-band feature is produced by 15, 15′-*cis*-spheroidene in WT RCs (Figure 7a, and inset).[8,12] Similar spectral differences between geometric isomers of open chain carotenoids have also been observed in solution at 77 K by Frank and co-workers.[36] The band peaking at 550 nm in the second EADS of

spheroidene-containing WT RCs (Figure 7a, red curve) is close to the peak of the $S_1 \rightarrow S_N$ transition of all-*trans*-spheroidene in LH2 complexes (shown in Figure 7b). The band at 570 nm reflects a new transition that has previously been associated with the *cis*-configuration (15, 15′-*cis*) of spheroidene in solution at 77 K.[36]

There are also resolvable spectral features other than the second peak at 570 nm. The EADS of both the hot and relaxed S_1 states from spheroidene-containing WT RCs exhibit large absorbance changes peaking at 625 and 615 nm, respectively (Figure 7a, inset, red and dark cyan curves). The strong absorption band at 625 nm in the second EADS (hot S_1) could be an enhanced vibrational band associated with the $S_1 \rightarrow S_N$ transition at 570 nm produced by the *cis*-configured spheroidene in the protein environment, as a similar vibrational band was also observed for the 15, 15′-*cis*- spheroidene in solution at 77 K.[36] However, the amplitude of this band is significantly stronger than that observed in solution. Note that contributions from the excited state absorption of the energy acceptor, B_B, are also possible in this spectral region (Figure 3b, green curve), but they decay on the subpicosecond time scale, and the extinction coefficient associated with these signals should be smaller than those of the carotenoid. The 610-nm band that occurs in the EADS representing the relaxed S_1 state is reminiscent of a "transient *cis* peak" identified as an $S_1 \rightarrow S_3$ transition in *cis*-configured carotenoids,[19] and is significantly enhanced in the protein environment, as well.

DISCUSSION

We have characterized excited state properties of the single carotenoid that resides within the RCs of the purple bacterium *Rb. sphaeroides*. Mutagenesis resulting in the loss of the primary electron donor, P, which is 11 Å from the carotenoid in WT,[8,9] introduces significant changes in the behavior of the carotenoid excited states in the VR(L157) mutant. The rates of energy transfer between the various carotenoid excited states and the energy acceptor, B_B, do not appear to change appreciably in the P-less mutant, as demonstrated by essentially the same S_2 and (relaxed) S_1 excited state dynamics in both mutant and WT RCs. However, the signals associated with the S* state in LH2 have counterparts in the P-less mutant, but not in WT RCs, and the intrinsic lifetime of the hot S_1 state appears to be shorter in the P-less mutant than in WT RCs. In addition, the P-less mutant has a hot S_1 lifetime similar to that observed in LH2 complexes.[23,34] Signals consistent with the formation of a long-lived carotenoid triplet state are also observed in the P-less mutant. The similarities between the P-less mutant and LH2 in terms of the carotenoid excited state properties, and the differences with respect to WT RCs, suggest that the carotenoid binding pocket in the P-less mutant is altered compared to that of WT RCs.

Effect of the Protein Environment on Carotenoid EET Pathways. EET between carotenoids and chlorophylls/bacteriochlorophylls has been extensively studied in various light-harvesting complexes from purple bacteria to higher plants (for reviews, see refs 2−4 and 27). The initially populated carotenoid S_2 state and the relaxed S_1 state are known to be the two major energy donating states. Their energy transfer efficiencies are thought to be relatively independent of their environment, depending instead on the conjugation length of the carotenoid backbone, which determines the energy levels of these two excited states.[2,3,27] The spectral and dynamic features observed here for the S_2 and S_1 excited states in WT and the P-less mutant are consistent with this view; while removal of P is expected to induce a significant change in the local environment, the properties of the S_2 and relaxed S_1 excited states are essentially unchanged. In contrast, the spectral evolution between the S_2 and S_1 states is altered. In both WT and the P-less mutant, there appears to be a vibrationally hot state (hot S_1 state) formed as an intermediate between S_2 and S_1. In WT RCs containing either spheroidene (Figure 7) or spheroidenone (Figure 3a), a high yield of hot S_1 state-mediated energy transfer is demonstrated by a large amplitude ground-state bleaching recovery that accompanies the decay of the hot S_1 excited-state absorbance. However, the amount of energy transferred from the hot S_1 state to B_B is lower in the P-less mutant (Figure 3b), and the observed hot S_1 state lifetime is shortened as compared to that in WT RCs. This suggests that it is the intrinsic vibrational relaxation time that has decreased in the P-less mutant.

Looking at this more quantitatively, the intrinsic relaxation time of the hot S_1 state τ_{Int}^{hotSl} in the absence of any energy transfer can be determined by solving the expression $\phi_{EET} = (1 - (\tau_{Obs})/\tau_{Int}^{hotSl}) \times 100$.[34] Given an energy transfer yield (ϕ_{EET}) of ∼60% for spheroidene in WT and a measured lifetime of τ_{Obs} = 680 fs (Table 1), a lifetime of $\tau_{Int}^{hotSl} \sim 1.7$ ps is obtained, which is more than double the lifetime of 700 fs reported for spheroidene with the same configuration (15,15′-*cis*) in solution at 77K.[36] One straightforward explanation for the retarded cooling process is that the motion of the carotenoid could be restricted in the protein binding pocket in WT RCs, making it more difficult to couple the excited state energy into local vibrational modes. This elongated intrinsic lifetime results in an increase in the yield of energy transfer in WT RCs from the carotenoid hot S_1 state to B_B. A similar estimation of the intrinsic relaxation time of the spheroidenone hot S_1 state in the VR(L157) RC results in a value of 0.6 ps, more than two times smaller than the WT RC value (Table 1). This decrease in the intrinsic relaxation time of the hot S_1 state is consistent with a reduction in the constraints of the carotenoid binding pocket, as proposed above and invoked to account for the appearance of the S* state in the P-less mutant (see discussion below). A less constrained carotenoid should result in enhanced coupling of the excited state to local vibrational modes and thus enhanced energy dissipation to the environment. Because the relaxation time is shorter, less energy transfer can occur from the hot S_1 state to B_B. It may be that in the LH2 complex, like in the P-less mutant, a decreased intrinsic lifetime results in less time for energy transfer. The crystal structures of LH2 and the photosystem I core complex from cyanobacteria and higher plants[43,44] suggest that there are probably more constraints on carotenoid motions from the protein environment of these systems than in LH2. This is consistent with the high energy transfer efficiency that is thought to occur from the hot S_1 state in these organisms.[45,46]

Carotenoid S* State in the RC Binding Pocket. The spectral and kinetic characteristics of the so-called S* state have been observed in increasing numbers of carotenoid-containing systems in recent studies.[19,32,35,47−50] The state appears to be more pronounced in protein environments than in solution. Moreover, the fate of the S* state varies, depending on the environment. The S* state has been identified in the LH1 complex from the photosynthetic bacterium *Rhodospirillum rubrum*. In this organism, the carotenoid involved is spirilloxanthin, which has a

conjugation length of 13 C=C double bonds,[37] and has been proposed to be a precursor of the carotenoid triplet state through a mechanism referred to as intramolecular homofission,[51] which is dependent on the time-dependent conformation of the carotenoid chain. Interactions between the carotenoid and the LH1 protein subunits are thought to lead to the dissociation of the singlet S* state into two triplets, resulting in nearly 30% triplet formation.[37] However, no triplet state was formed from the same molecule in solution,[37] and a much lower yield of 5−10% was detected when spirilloxanthin was reconstituted into the LH2 apoprotein from *Rb. sphaeroides*.[52] In the latter system, the S* state was observed to transfer its energy to the nearby bacteriochlorophylls. These results suggest that both the formation and decay of the S* state are dependent on the conformation of the carotenoid in the binding pocket and/or its interaction with the protein.

One of the novel observations in this study is that a state with S*-like spectral and kinetic features was observed in RCs from the P-less mutant, but not in WT RCs. In any case, kinetically, a description of the carotenoid excited state evolution in the P-less mutant RC in terms of a series of sequential intermediates requires the introduction of a long-lived state (Figure 3b), which is similar in important respects to the S* state observed previously in light-harvesting systems. As discussed above in terms of the hot S_1 relaxation analysis, there appear to be fewer structural constraints on the carotenoid imposed by the protein binding pocket in the P-less mutant than in WT RCs. It is possible that the more relaxed protein constraints on the configuration of the carotenoid in the P-less mutant also facilitate the formation of the S* state. This is consistent with previous proposals that S* state formation is correlated with carotenoid deformation.[19,37] In this model, the steric constraints placed on the carotenoid backbone in the binding pocket of WT RCs would be sufficient to inhibit the degree of twisting or deformation in the singlet excited states required for the S* state formation.

A structural comparison of the carotenoid binding pocket in WT RCs and LH2 is potentially instructive in this regard, as the S* state spectral and kinetic signatures are best characterized in LH2,[21,23,34] and the carotenoid signals in the P-less mutant are similar to those of LH2 and quite distinct from WT RCs. The 15,15′-*cis*-configuration carotenoid in the RC lies in a plane roughly parallel to the surface of the membrane (Figure 1). It is located entirely within the M subunit in the RC complex and bends sharply in the vicinity of the two *trans*-membrane helices.[8] The conjugated polyene portion of the carotenoid is stabilized by $\pi-\pi$ stacking interactions at several regions with aromatic amino acid residues, and with B_B. A structural comparison of RCs reconstituted with three spheroidene analogues revealed a well-conserved region located near the central 15, 15′-*cis* bond,[8] which is stabilized by both the macrocycle and phytol tail of B_B.[8] In LH2, there are fewer numbers of aromatic amino acid residues within the binding pocket to provide interactions with the carotenoid backbone than in RCs.[12] Similar stabilization interactions from the bacteriochlorophyll phytol tail to the carotenoid are not observed, although the central part of the carotenoid backbone is also in van der Waals contact with the macrocycle of the monomer B800-bacteriochlorophyll molecule. In the VR(L157) mutant, the conformational restrictions of the carotenoid could be disturbed due to the loss of the P-forming bacteriochlorophyll molecules.

Carotenoid Triplet State Observed in the P-less Mutant RC. The nondecaying component in the global analysis of the transient absorption data from VR(L157) mutant RCs (Figure 3b and inset, black curve) is most simply interpreted as the carotenoid triplet state. It has an absorption increase peaking at ∼610 nm, similar to the broad 600 nm absorbance increase that has been observed previously from nanosecond laser flash photolysis measurements on spheroidenone-containing bacterial RCs by Arellano and co-workers.[40]

Given the small amplitude of the S* signal in the VR(L157) mutant (Figure 5), and the maximum yield of 30% reported for the S*-to-triplet state conversion in previous studies,[35,37] the amplitude of the final triplet carotenoid signal in Figure 3b appears too large to have formed predominantly via the spheroidenone S* state. Instead, the carotenoid triplet state is likely formed as a result of triplet energy transfer from B_B. In this mutant, long-lived B_B* presumably generates triplet B_B via intersystem crossing or charge recombination that rapidly transfers the triplet excitation to the carotenoid. This is the second half of the two-step mechanism proposed for the photoprotective function of *cis*-configured carotenoid in purple bacterial RCs, in which quenching of triplet P is thought to occur through triplet energy transfer to the carotenoid via B_B.[13] The regeneration of carotenoid ground-state bleaching on the nanosecond time scale (Figure 6), as B_B* associated absorbance changes decay, is consistent with such a pathway. This conclusion is further supported by the observation that the same long-lived carotenoid state is observed when B_B was excited directly at 590 nm in the P-less mutant (data not shown). In that case, both bacteriochlorophyll monomers (B_A and B_B) are excited, but not the carotenoid. While it has long been thought that such a pathway for triplet quenching is used by bacterial RCs, this provides the most direct evidence for triplet−triplet energy transfer from B_B to the *cis*-configured RC carotenoid to date. In WT RCs, no triplet is observed via this pathway because almost all of the B_B* state formed is quenched by P, and in the experiments described here, P^+ (Figure 4).

CONCLUDING REMARKS

The protein environment appears to play an important role in determining the excited state properties of the carotenoid in photosynthetic complexes. In this study, the rate of vibrational relaxation is quite sensitive to mutagenically induced changes in the protein, suggesting that there are specific protein interactions that are designed to decrease the coupling between carotenoid excited states and local vibrational modes in the environment, in this case enhancing the overall yield of energy transfer in the WT system between the carotenoid and the local bacteriochlorophylls. Similarly, pathways of interconversion between carotenoid excited states are also apparently controlled. Specifically in RCs, a long-lived state similar to the S* state observed in LH2 appears only in a mutant that likely alters the carotenoid environment − again fairly specific aspects of the carotenoid−protein interaction change the evolution of the excited state. This is just one more example of how proteins function to control chemistry. Past work has already given numerous examples of protein control of electron transfer rate and pathway in RCs on ultrafast time scales.[53−55] In the current work, direct and specific control of the excited state properties of a RC cofactor by protein interactions is characterized. Finally, by manipulating the interaction between the carotenoid excited states, neighboring cofactors, and the protein environment, it has been possible to modulate not only singlet energy transfer from the carotenoid

to neighboring bacteriochlorophyll molecules, but also triplet transfer from bacteriochlorophyll to the carotenoid, opening the door for future studies of photoprotection mechanisms.

AUTHOR INFORMATION

Corresponding Author
*E-mail: Jie.Pan.1@asu.edu and Slin@asu.edu.

ACKNOWLEDGMENT

The authors thank Prof. Tomáš Polívka for helpful discussions. J.P. thanks Dr. Mikas Vengris at Vilnius University, Lithuania, for kindly providing the global analysis fitting program. This research was supported by NSF Grants MCB0642260 and MCB0640002 at ASU. Work in the laboratory of H.A.F. was supported by NSF Grant MCB-0913022 and the University of Connecticut Research Foundation. The transient spectrometer used was funded by NSF Grant BIR9512970.

REFERENCES

(1) Frank, H. A.; Cogdell, R. J. In *Carotenoids in Photosynthesis*; Young, A. J., Britton, G., Eds.; Chapman & Hall: London, 1993, p 252.
(2) Polivka, T.; Sundstrom, V. *Chem. Rev.* **2004**, *104*, 2021.
(3) Polivka, T.; Frank, H. A. *Acc. Chem. Res.* **2010**, *43*, 1125.
(4) Vaswani, H. M.; Holt, N. E.; Fleming, G. R. *Pure Appl. Chem.* **2005**, *77*, 925.
(5) Frank, H. A.; Bautista, J. A.; Josue, J.; Pendon, Z.; Hiller, R. G.; Sharples, F. P.; Gosztola, D.; Wasielewski, M. R. *J. Phys. Chem. B* **2000**, *104*, 4569.
(6) Polivka, T.; Pellnor, M.; Melo, E.; Pascher, T.; Sundstrom, V.; Osuka, A.; Naqvi, K. R. *J. Phys. Chem. C* **2007**, *111*, 467.
(7) Zigmantas, D.; Hiller, R. G.; Sharples, F. P.; Frank, H. A.; Sundstrom, V.; Polivka, T. *Phys. Chem. Chem. Phys.* **2004**, *6*, 3009.
(8) Roszak, A. W.; McKendrick, K.; Gardiner, A. T.; Mitchell, I. A.; Isaacs, N. W.; Cogdell, R. J.; Hashimoto, H.; Frank, H. A. *Structure* **2004**, *12*, 765.
(9) Yeates, T. O.; Komiya, H.; Chirino, A.; Rees, D. C.; Allen, J. P.; Feher, G. *Proc. Natl. Acad. Sci. U.S.A.* **1988**, *85*, 7993.
(10) Woodbury, N. W.; Allen, J. P. *In Anoxygenic Photosynthetic Bacteria*; Kluwer Academic Publishers: Dordrecht, The Netherlands, 1995; Vol. 2.
(11) Cogdell, R. J.; Gall, A.; Kohler, J. *Q. Rev. Biophys.* **2006**, *39*, 227.
(12) McDermott, G.; Prince, S. M.; Freer, A. A.; Hawthornthwaite-lawless, A. M.; Papiz, M. Z.; Cogdell, R. J.; Isaacs, N. W. *Nature* **1995**, *374*, 517.
(13) deWinter, A.; Boxer, S. G. *J. Phys. Chem. B* **1999**, *103*, 8786.
(14) Lin, S.; Katilius, E.; Ilagan, R. P.; Gibson, G. N.; Frank, H. A.; Woodbury, N. W. *J. Phys. Chem. B* **2006**, *110*, 15556.
(15) Lin, S.; Katilius, E.; Taguchi, A. K. W.; Woodbury, N. W. *J. Phys. Chem. B* **2003**, *107*, 14103.
(16) Jones, M. R. Structural Plasticity of Reaction Centers from Purple Bacteria. In *The Purple Phototrophic Bacteria*; Hunter, C. N., Daldal, F., Thurnauer, M. C., Beatty, J. T., Eds.; Advances in Photosynthesis and Respiration; Springer: Dordrecht, The Netherlands, 2009; p 295.
(17) Williams, J. C.; Allen, J. P. Directed Modification of Reaction Centers from Purple Bacteria. In *The Purple Phototrophic Bacteria*; Hunter, C. N., Daldal, F., Thurnauer, M. C., Beatty, J. T., Eds.; Advances in Photosynthesis and Respiration; Springer: Dordrecht, The Netherlands, 2009; p 337.
(18) de Weerd, F. L.; van Stokkum, I. H. M.; van Grondelle, R. *Chem. Phys. Lett.* **2002**, *354*, 38.
(19) Niedzwiedzki, D.; Koscielecki, J. F.; Cong, H.; Sullivan, J. O.; Gibson, G. N.; Birge, R. R.; Frank, H. A. *J. Phys. Chem. B* **2007**, *111*, 5984.
(20) Billsten, H. H.; Sundstrom, V.; Polivka, T. *J. Phys. Chem. A* **2005**, *109*, 1521.
(21) Wohlleben, W.; Buckup, T.; Herek, J. L.; Cogdell, R. J.; Motzkus, M. *Biophys. J.* **2003**, *85*, 442.
(22) Papagiannakis, E.; van Stokkum, I. H. M.; Vengris, M.; Cogdell, R. J.; van Grondelle, R.; Larsen, D. S. *J. Phys. Chem. B* **2006**, *110*, 5727.
(23) Papagiannakis, E.; Kennis, J. T. M.; van Stokkum, I. H. M.; Cogdell, R. J.; van Grondelle, R. *Proc. Natl. Acad. Sci. U.S.A.* **2002**, *99*, 6017.
(24) Polivka, T.; Sundstrom, V. *Chem. Phys. Lett.* **2009**, *477*, 1.
(25) Koyama, Y.; Rondonuwu, F. S.; Fujii, R.; Watanabe, Y. *Biopolymers* **2004**, *74*, 2.
(26) Rondonuwu, F. S.; Yokoyama, K.; Fujii, R.; Koyama, Y.; Cogdell, R. J.; Watanabe, Y. *Chem. Phys. Lett.* **2004**, *390*, 314.
(27) Frank, H. A.; Polivka, T. Energy Transfer from Carotenoids to Bacteriochlorophylls. In *The Purple Phototrophic Bacteria*; Hunter, C. N., Daldal, F., Thurnauer, M. C., Beatty, J. T., Eds.; Advances in Photosynthesis and Respiration; Springer: Dordrecht, The Netherlands, 2009; p 213.
(28) Jackson, J. A.; Lin, S.; Taguchi, A. K. W.; Williams, J. C.; Allen, J. P.; Woodbury, N. W. *J. Phys. Chem. B* **1997**, *101*, 5747.
(29) Goldsmith, J. O.; Boxer, S. G. *Biochim. Biophys. Acta, Bioenerg.* **1996**, *1276*, 171.
(30) Katilius, E.; Babendure, J. L.; Lin, S.; Woodbury, N. W. *Photosynth. Res.* **2004**, *81*, 165.
(31) Gradinaru, C. C.; van Stokkum, I. H. M.; Pascal, A. A.; van Grondelle, R.; van Amerongen, H. *J. Phys. Chem. B* **2000**, *104*, 9330.
(32) Jailaubekov, A. E.; Song, S.-H.; Vengris, M.; Cogdell, R. J.; Larsen, D. S. *Chem. Phys. Lett.* **2010**, *487*, 101.
(33) van Stokkum, I. H. M.; Larsen, D. S.; van Grondelle, R. *Biochim. Biophys. Acta, Bioenerg.* **2004**, *1657*, 82.
(34) Cong, H.; Niedzwiedzki, D. M.; Gibson, G. N.; LaFountain, A. M.; Kelsh, R. M.; Gardiner, A. T.; Cogdell, R. J.; Frank, H. A. *J. Phys. Chem. B* **2008**, *112*, 10689.
(35) Polivka, T.; Balashov, S. P.; Chabera, P.; Imasheva, E. S.; Yartsev, A.; Sundstrom, V.; Lanyi, J. K. *Biophys. J.* **2009**, *96*, 2268.
(36) Niedzwiedzki, D. M.; Sandberg, D. J.; Cong, H.; Sandberg, M. N.; Gibson, G. N.; Birge, R. R.; Frank, H. A. *Chem. Phys.* **2009**, *357*, 4.
(37) Gradinaru, C. C.; Kennis, J. T. M.; Papagiannakis, E.; van Stokkum, I. H. M.; Cogdell, R. J.; Fleming, G. R.; Niederman, R. A.; van Grondelle, R. *Proc. Natl. Acad. Sci. U.S.A.* **2001**, *98*, 2364.
(38) Frank, H. A.; Chynwat, V.; Posteraro, A.; Hartwich, G.; Simonin, I.; Scheer, H. *Photochem. Photobiol.* **1996**, *64*, 823.
(39) Fujii, R.; Furuichi, K.; Zhang, J. P.; Nagae, H.; Hashimoto, H.; Koyama, Y. *J. Phys. Chem. A* **2002**, *106*, 2410.
(40) Arellano, J. B.; Melo, T. B.; Fyfe, P. K.; Cogdell, R. J.; Naqvi, K. R. *Photochem. Photobiol.* **2004**, *79*, 68.
(41) Zhang, J. P.; Fujii, R.; Qian, P.; Inaba, T.; Mizoguchi, T.; Koyama, Y.; Onaka, K.; Watanabe, Y.; Nagae, H. *J. Phys. Chem. B* **2000**, *104*, 3683.
(42) Walla, P. J.; Linden, P. A.; Hsu, C. P.; Scholes, G. D.; Fleming, G. R. *Proc. Natl. Acad. Sci. U.S.A.* **2000**, *97*, 10808.
(43) Jordan, P.; Fromme, P.; Witt, H. T.; Klukas, O.; Saenger, W.; Krauss, N. *Nature* **2001**, *411*, 909.
(44) Liu, Z. F.; Yan, H. C.; Wang, K. B.; Kuang, T. Y.; Zhang, J. P.; Gui, L. L.; An, X. M.; Chang, W. R. *Nature* **2004**, *428*, 287.
(45) Hilbert, M.; Wehling, A.; Schlodder, E.; Walla, P. J. *J. Phys. Chem. B* **2004**, *108*, 13022.
(46) Walla, P. J.; Linden, P. A.; Ohta, K.; Fleming, G. R. *J. Phys. Chem. A* **2002**, *106*, 1909.
(47) Wohlleben, W.; Buckup, T.; Hashimoto, H.; Cogdell, R. J.; Herek, J. L.; Motzkus, M. *J. Phys. Chem. B* **2004**, *108*, 3320.
(48) Chabera, P.; Fuciman, M.; Hribek, P.; Polivka, T. *Phys. Chem. Chem. Phys.* **2009**, *11*, 8795.
(49) Zhu, J. Y.; Gdor, I.; Smolensky, E.; Friedman, N.; Sheves, M.; Ruhman, S. *J. Phys. Chem. B* **2010**, *114*, 3038.
(50) Berera, R.; van Stokkum, I. H. M.; Kodis, G.; Keirstead, A. E.; Pillai, S.; Herrero, C.; Palacios, R. E.; Vengris, M.; van Grondelle, R.;

Gust, D.; Moore, T. A.; Moore, A. L.; Kennis, J. T. M. *J. Phys. Chem. B* **2007**, *111*, 6868.
(51) Tavan, P.; Schulten, K. *Phys. Rev. B* **1987**, *36*, 4337.
(52) Papagiannakis, E.; Das, S. K.; Gall, A.; van Stokkum, I. H. M.; Robert, B.; van Grondelle, R.; Frank, H. A.; Kennis, J. T. M. *J. Phys. Chem. B* **2003**, *107*, 5642.
(53) Wang, H. Y.; Lin, S.; Allen, J. P.; Williams, J. C.; Blankert, S.; Laser, C.; Woodbury, N. W. *Science* **2007**, *316*, 747.
(54) Pawlowicz, N. P.; Van Grondelle, R.; van Stokkum, I. H. M.; Breton, J.; Jones, M. R.; Groot, M. L. *Biophys. J.* **2008**, *95*, 1268.
(55) Lee, H.; Cheng, Y. C.; Fleming, G. R. *Science* **2007**, *316*, 1462.